Sensitivity of reservoir and operational parameters on the energy extraction performance of combined CO_2-EGR–CPG systems

Justin Ezekiel[a], Diya Kumbhat[a], Anozie Ebigbo[a,b], Benjamin M. Adams[a], Martin O. Saar[a,c]

[a]*Geothermal Energy and Geofluids Group, Department of Earth Sciences, ETH Zurich, Sonneggstrasse 5, 8092 Zurich, Switzerland*

[b]*Hydromechanics Group, Helmut Schmidt University, Hamburg, Holstenhofweg 85, 22043 Hamburg, Germany*

[c]*Department of Earth and Environmental Sciences, University of Minnesota, 116 Church Street SE, Minneapolis, USA*

Abstract

There is a potential for synergy effects in utilizing CO_2 for both enhanced gas recovery (EGR) and geothermal energy extraction (CO_2-plume geothermal, CPG) from natural gas reservoirs. This "combined CO_2-EGR–CPG system" has been introduced as a feasible approach that constitutes a CO_2 Capture double-Utilization and Storage (CCUUS) system. In this study, we carry out reservoir simulations, using TOUGH2, to evaluate the sensitivity of the natural gas recovery, pressure buildup, and geothermal power generation performance of the combined system to various key reservoir and operational parameters. The reservoir parameters include horizontal permeability, permeability anisotropy, reservoir temperature, and pore-size-distribution index; while the operational parameters include wellbore diameter and ambient surface temperature. Using an example of a natural gas reservoir model, we also investigate the effects of different strategies of transitioning from the CO_2-EGR stage to the CPG stage on the energy-recovery performance metrics and on the two-phase fluid-flow regime in the production well.

The simulation results show that overlapping the CO_2-EGR and CPG stages and having a relatively brief period of CO_2 injection but no production (which we call the CO_2-plume establishment stage) achieves the best overall energy (natural gas and geothermal) recovery performance. Permeability anisotropy and reservoir temperature are the parameters the natural gas recovery performance of the combined system is most sensitive to. The geothermal power generation performance is most sensitive to the reservoir temperature and the production wellbore diameter. The results of this study pave the way for future CPG-based geothermal power-generation optimization studies. For a CO_2-EGR–CPG project, the results can be a guide regarding the required accuracy of the reservoir parameters during exploration and data acquisition.

Keywords: CO_2-plume geothermal (CPG), Enhanced gas recovery (EGR), Combined CO_2-EGR–CPG system, Sensitivity analysis, Reservoir simulation, Geothermal power generation.

1. Introduction

The effects of global warming on the environment (including sea level rise, extreme weather conditions, etc.) are on the rise due to anthropogenic emissions of greenhouse gases, mostly carbon dioxide (CO_2). The development and use of clean, low-carbon, energy-efficient technologies and renewable energy sources are ways of reducing such emissions. To this effect, the technology, known as Carbon Capture and Storage (CCS), which features the capture of CO_2 from flue gases of power plants (and other large CO_2-emitting industrial plants) and storage in suitable, carefully selected geological formations, is widely considered part of the technologies needed to achieve net-zero CO_2 emissions [1–3].

The coupling of CCS to the industrial utilization of the captured CO_2, termed Carbon Capture, Utilization and Storage (CCUS) can reduce its costs. CCUS is expected to contribute 9% of the cumulative emissions reduction before 2050 [2,4], to meet the goal of limiting the average global temperature rise to 1.5 °C. Hence, the widespread use and deployment of CCUS technologies is important [2]. Depleted gas reservoirs are considered one of the prime candidates for the storage of CO_2 due to the integrity and safety benefits that such sites provide. CO_2 injection into partially depleted or depleted natural gas reservoirs can enhance the production of the gas (enhanced gas recovery, EGR), which is a typical example of combining CO_2 utilization and storage.

CO_2 injection into natural gas reservoirs has been studied for CO_2 storage and EGR [5–8]. Published studies on the injection of CO_2 into depleted gas reservoirs with the purpose of improving gas recovery and storing CO_2 go as far back as three decades [9,10]. Examples of pilot projects of CO_2 injection into depleted natural gas reservoirs include the CO_2-EGR project in the Budafa Szinfelleti field in Hungary [11,12]; the CO_2-EGR and CO_2 storage project in the K12-B depleted gas field in the Netherlands [13,14]; and the CLEAN project in the Altmark gas field in Germany [15–17]. Feasibility studies (numerical simulations and laboratory experiments) of CO_2-EGR in natural gas reservoirs have been carried out using geological data from gas fields in different countries including the Netherlands [8,13,14], USA [18–20], Germany [15–17,21,22], Italy [23], Austria [7,24,25], Australia [26,27], and China [28,29]. Results from various studies show that significant amounts of additional natural gas can be recovered through CO_2-EGR [5,8,22,27]. Numerical simulation results also show that injecting CO_2 at the bottom of the reservoir and extracting methane from the top ensures that the denser CO_2 remains below the methane, which minimizes CO_2 upconing at the production well [5,18]. Eventually, when a mixed gas of methane and CO_2 is produced at the land surface, CO_2 can be separated with amine solvents or membranes recovering up to 97% pure methane [30,31]. The separated CO_2 can be reinjected into the reservoir so that all of the initially injected CO_2 is eventually stored underground, resulting in true CCUS, i.e. one where the CO_2 is both utilized and completely stored.

Furthermore, geothermal energy development has been regarded as one of the promising renewable energy options which can contribute to the reduction of global dependence on fossil-fuel, non-renewable energy sources [32–34]. It has also been proposed that using supercritical carbon dioxide ($scCO_2$), in place of the traditional water or brine, as the subsurface heat-transmission working fluid to develop geothermal energy, comes with added benefits [35–38]. Due to the favorable heat-extraction properties of CO_2 (i.e. high thermal expansivity and low kinematic viscosity) compared to subsurface water/brine, low- and medium-enthalpy geothermal reservoirs can be utilized more efficiently when employing supercritical CO_2 as the subsurface working fluid than when groundwater or brine are used. The low kinematic viscosity of CO_2 leads to high injectivity into, and high flowrate through, the geothermal reservoir, given a fluid-pressure gradient from the injection to the production well. The high fluid flowrates of CO_2 compared to water for a given fluid pressure gradient result in correspondingly higher advective heat transfer and thus energy-extraction rates for CO_2 versus water, all else being equal [39,40]. The high thermal expansivity of supercritical CO_2 results in a buoyancy-driven thermosiphon, which minimizes or eliminates parasitic pumping requirements of the CO_2-based geothermal energy system [35,38–41].

CO_2-based geothermal power generation was initially considered for Enhanced Geothermal Systems (EGS) [35,37,42,43], which involves hydraulically stimulating (fracturing or shearing) crystalline rocks to create flow paths for the injected CO_2. However, EGS comes with the disadvantages of limited spatial extent, and thus a rather limited energy resource, and induced seismicity [44,45] Over the last decade, the concept – called CO_2 Plume Geothermal (CPG) – of injecting CO_2 into sedimentary reservoirs (for example deep aquifers or hydrocarbon reservoirs) overlain by a low-permeability caprock has been featured more prominently in research [38–40,46–51]. During CPG, instead of only storing CO_2 in sedimentary basins (i.e. conducting only CCS), the injected CO_2 is additionally circulated back to the land surface and used to generate power in a CO_2 turbomachinery. The produced CO_2 is reinjected, and all the injected CO_2 is permanently stored in the same reservoir. CPG is thus an example of a CCUS system.

The above research on CPG has thus far focused on deep saline formations as CPG-host reservoirs. However, Refs. [49,50,52] have investigated hydrocarbon reservoirs as CPG hosts, as, for example, hot natural gas reservoirs have been shown to contain not only natural gas resources but significant geothermal energy reserves. In fact, we have presented, in Ref. [49], the potential for extracting heat from produced natural gas and utilizing $scCO_2$ as a subsurface working fluid for the dual purpose of enhancing gas recovery (CO_2-EGR) and extracting geothermal energy (CPG) from deep, hot natural gas reservoirs for electric power generation, while ultimately storing all of the subsurface-injected CO_2. This approach of using the subsurface CO_2 both for enhancing natural gas recovery and for extracting geothermal energy, while ultimately storing all of the CO_2 underground, a combined CO_2-EGR–CPG system, constitutes a CO_2 Capture double-Utilization and Storage (CCUUS) system. The advantages associated with this combined system have been discussed in detail in Ref. [49] and Ref. [52]. Some of these main advantages include:

(i) The combined system exhibits less pore-water influence (due to the presence of residual natural gas), which could make it possible for the CO_2 to flow as a single phase in the reservoir. This also reduces complicated CO_2-rock-water interactions and makes the system more attractive and efficient for CO_2-based geothermal energy extraction than other (mostly water-bearing) sedimentary geothermal reservoirs.

(ii) Additional natural gas and geothermal energy are extracted for power generation, which leads to an increase in the gas field's total amount of producible energy.

(iii) The natural-gas-based power generation would very likely be operated with CCS, providing the CO_2 to the EGR and later the CPG operations, while eliminating CO_2 emissions from the natural-gas-based power generation.

(iv) Economic (cost-saving) benefits are achieved by using/sharing already-existing multidisciplinary datasets (on reservoir parameters) and infrastructure (surface facilities, wells, etc.). Hence, investment costs are significantly reduced.

(v) The combined system extends the useful lifetime of the gas reservoir, recovering otherwise stranded assets such as wells, offshore platforms, etc., thereby postponing the expensive decommissioning phase of the wells and abandonment stages of the gas field.

Different stages have been identified for energy (and power) generation from the combined system (see also Ref. [49]). These stages include the conventional natural gas recovery (CNGR) stage, where natural gas is produced by the primary recovery drive and at the surface, the associated heat is extracted and converted to power using an Organic Rankine cycle (ORC) or a CO_2-based Rankine cycle (CRC). The CNGR stage is followed by the CO_2-EGR stage when the fluid pressure or natural gas has been depleted and the remaining natural gas cannot be economically recovered by just the natural primary drive. CO_2 is injected into the reservoir to recover the remaining natural gas and reduce the residual methane content in the reservoir. The associated heat in the produced and remaining natural gas is extracted and converted to power as described above. At some point during the CO_2-EGR stage, CO_2 breakthrough occurs in the production well. Hence, the installation of a methane-CO_2 separator is required at the surface.

A transition period (TP) exists at the CO_2-EGR stage before the CPG stage begins. It is the period when the mass fraction of CO_2 in the produced fluid is greater than 10% and less than 90%. We assume that the separation of the produced mixed fluid is necessary. The separation process of CO_2 and methane (CH_4) is cost- and energy-intensive, requiring higher energy input than the geothermal power generated during the CO_2-EGR stage. The longer this "transition period" lasts, the higher is the parasitic power required to separate the mixed fluid at the surface. However, during this transition period, the heat in the separated methane can be extracted and converted to power using the indirect power system, if desired. The separated CO_2 is not used for energy extraction and is simply reinjected into the reservoir.

Ref. [49] describes a CO_2-plume establishment (PE) stage, where the production well is shut-in and CO_2 injection is continued to charge the reservoir with CO_2 and establish a CO_2 plume between the injection and the production wells. The PE stage can come before or after the CO_2-EGR stage (the latter is the case in the simulations shown later), depending on the operational strategy.

After the transition period, the CPG stage commences and all produced fluid (mostly CO_2) is sent to the direct CO_2 turbine for direct-CPG [40,47,48] power generation. Our reservoir simulation results for the CPG stage show that, using a scalable reservoir-model example, a CO_2-circulation mass flowrate of 110 kg/s results in a maximum power output of 2 MW_e using the direct CPG power plant [49]. This power output is about 4 times the power that would be generated if the indirect (ORC or CRC) power system is used instead (see also Ref. [40]). The CO_2 leaving the turbine is further cooled and reinjected into the reservoir. When the reservoir heat is depleted, after decades as shown in Ref. [47,48], the CPG-based injection and production wells are shut down and the injected CO_2 is permanently stored in the natural gas reservoir.

In this study, we use a similar anticlinal natural gas reservoir model as described in Ref. [49], to carry out reservoir simulations (in TOUGH2 [53,54]), aimed at expanding the previous study on the combined CO_2-EGR–CPG system to:

(i) accommodate lessons learned from Ref. [55], including that the bottom-hole production flowrate directly influences how much water enters the production well and that the two-phase (water/CO_2) flow regime in the production well is an important design parameter;
(ii) determine the effect of the residual CH_4 content of the reservoir, the effect of the CO_2-plume-establishment stage, and the effects of the different reservoir and operational (non-reservoir) parameters on the natural gas recovery, pressure buildup, and the electric power generation of the combined system.

This study focuses on determining how sensitive the performance metrics (mentioned in the above points (i) and (ii) of the combined system) are to some key reservoir and operational parameters. It also provides a preliminary guide for identifying the favorable factors in selecting suitable natural gas reservoirs and the most effective implementation strategy for the combined CO_2-EGR–CPG system.

2. Methodology

In this section, we describe the natural gas model, numerical simulation, and performance metrics used for this study. We report the changes we have made to the original natural gas reservoir model (presented in Ref. [49]) and the implementation strategy/concept of the combined system for effective natural gas and geothermal energy extraction from the natural gas reservoir. We describe the numerical model we use to simulate the three main stages (CNGR, CO_2-EGR+TP, and CPG stages) associated with the combined system. Finally, we explain how the sensitivity study is conducted.

2.1 Reservoir modeling and simulation

2.1.1 Modified reservoir model (after Ref. [49])

Using some of the reservoir properties of some examples of hot/deep natural gas fields in the world, we set up a similar natural gas reservoir to that of our previous study (see Figure 2.2 of Ref. [49]), in terms of model geometry, well configuration, boundary conditions, and relative permeability functions. However, the fluid properties of the current model are updated such that the salt concentration changes from zero in the previous model to 150,000 ppm in the current model. Furthermore, the y-axis dimension of the full model is extended from previously 3 km to now 4.5 km, so that the updated model has equal dimensions on all sides. We also introduce a horizontal to vertical permeability anisotropy of kh/kv = 2 in the base-case model. We carry out our simulations using the same reservoir simulator, TOUGH2 with the EOS7C module, developed for simulating gas and brine flow as well as heat transport in (natural gas) reservoirs [53,54]. The rock and fluid properties of the new model as well as the initial conditions are summarized in Table 1.

2.1.2 Reservoir simulation schemes

Based on the model of the combined CO_2-EGR-CPG described above, the numerical simulations are carried out in three main stages:

a) The CNGR stage with a base-case duration of 25 years at a production flowrate of 4 kg/s/well.
b) The CO_2-EGR stage with all simulated cases lasting for 1 year with a high injection-production flowrate ratio [49,52] (i.e. injection flowrate of 30 kg/s/well and production flowrate of 4 kg/s/well). The high injection-production flowrate ratio is beneficial for achieving a good CO_2-EGR performance as well as a short duration for establishing an adequate CO_2-plume reservoir [52]. After the 1-year period of high injection-production flow rate ratio, the production rate is increased to 30 kg/s/well (equal to the injection flow rate). The CO_2-EGR stage ends when the mass fraction of CO_2 (XCO_2) at the production well region has reached 90%. In this study, we consider some cases that are associated with 1.5 years of CO_2-plume establishment (PE) stage after the 1-year CO_2-EGR stage. After the PE stage, the transition period, which involves CO_2-CH_4 separation, continues till 90% CO_2 mass fraction (in the gas phase) is reached at the production well region.
c) Finally, there is the CPG stage. The base-case CPG-stage duration is 30 years at a circulation flow rate of 30 kg/s/well.

2.2 Performance metrics

In this section, we present how we calculate the metrics used to measure the energy-extraction performance for the different cases considered in this study. These metrics include:

(a) the CO_2 saturation (in the reservoir and in the well), and the corresponding flow regime established (at the bottom-hole section of the production well) at the time of highest water saturation around the production-well inlet region of the reservoir (Ref. [49]). This performance metric is only applicable for the reservoir parameters, and it can be used to determine the importance of the PE stage for the combined system to achieve an annular flow regime (dominant CO_2 flow) in the production well. The method to calculate this metric, using the gas saturation in the well and flow rate, can be found in Ref. [55].

Table 1: Parameters for the base-case reservoir model

Parameter	Value
Reservoir size, x (km), y (km), z (km)	4.5 x 4.5 x 0.1
Depth (km)	3.0
Porosity (-)	0.20
Horizontal permeability, kh (m^2)	10^{-13} (100 mD)
Anisotropy k_h/k_v (-)	2.0
Thickness (m)	100
Reservoir initial pressure	Hydrostatic (30 MPa at the top of the reservoir)
Reservoir initial temperature (°C)	120
Initial CO_2 mass fraction in gas phase	0.025 (dissolved in brine)
Residual gas saturation (-)	0.05
Residual brine saturation (-)	0.25
van Genuchten parameters α (Pa), *m* (-)	$3x10^3$, 0.77
Native brine NaCl saturation (ppm)	150,000
Mol. diffusivity in gas; in water (m^2/s)	10^{-5}; 10^{-10}
Rock grain density (kg/m^3)	2650
Thermal conductivity λ_{wet}, λ_{dry} (W/m°C)	2.51, 1.6
Rock specific heat capacity (J/kg°C)	1000
Geothermal gradient (°C/km)	35
Rock compressibility (1/Pa)	10^{-10}
CO_2 injection enthalpy (J/kg)	$2.8x10^5$
Well diameter (m)	0.14
Lateral boundary conditions of the reservoir	Hydrostatic pressure; 120°C (Dirichlet boundary conditions).
Top and bottom boundary conditions of the reservoir	No fluid flow and no heat flux.

(b) the natural gas recovery performance (NGRP), which incorporates the amount of natural gas recovered (in terms of natural gas recovery factor) and the duration of the CNGR and CO_2-EGR stages (including the transition period (TP), i.e. the period before the CO_2 mass fraction of the produced gas reaches 90%). This implies that the duration of natural gas recovery would also include the time of CH_4-CO_2 separation at the land surface. The natural gas recovery factor during the CNGR and CO_2-EGR stages can be measured as a percentage of the original gas in place (OGIP). These respective factors are calculated as

$$\text{CNGR factor, } F_{\text{CNGR}}\ (\%) = \frac{V_{g-\text{CNGR}}}{\text{OGIP}} \cdot 100, \qquad (1)$$

where $V_{g-\mathrm{CNGR}}$ is the volume of gas produced during the CNGR stage, OGIP is the volume of gas initially in place,

$$\text{EGR factor, } F_{\mathrm{EGR}}\ (\%) = \frac{V_{g-\mathrm{EGR}}}{\mathrm{OGIP}} \cdot 100, \tag{2}$$

where $V_{g-\mathrm{EGR}}$ is the volume of gas produced during the CO_2-EGR stage, and

$$\text{Ultimate recovery factor, } F_{\mathrm{UR}}\ (\%) = F_{\mathrm{CNGR}} + F_{\mathrm{EGR}}\ . \tag{3}$$

The volumes of the produced gas during the CNGR and CO_2-EGR stages can be obtained from the TOUGH2 simulation output files.

The natural gas recovery performance is measured using a natural gas recovery index (RI), which is calculated as the ultimate recovery factor [%] divided by the sum of the durations of the CNGR stage, t_{CNGR} [year] and CO_2-EGR+TP stage, t_{EGR} [year] (Equation 4).

$$\mathrm{RI}\ (\%/\mathrm{year}) = {F_{\mathrm{UR}}}/{(t_{\mathrm{CNGR}} + t_{\mathrm{EGR+TP}})}\ . \tag{4}$$

The recovery index provides a way to select the best reservoir parameters and strategies that favor natural gas recovery and a shorter duration of the CO_2-CH_4 separation. The shorter this transition period is, the higher is the energy efficiency of the combined system. Hence, a high value of RI is favorable.

(c) the pressure buildup, at the injection wells, is one of the performance metrics considered for the combined system. This important high-pressure buildup (overpressure) at the injection wells can influence the integrity of the caprock overlying the natural gas reservoir. The non-dimensional pressure buildup (PBU) metric, used in this study, compares the maximum pressure in the injection well, $P_{\mathrm{wb-max}}$, to the initial reservoir pressure, P_0, as shown in Equation (5).

$$\mathrm{PBU} = \frac{P_{\mathrm{wb-max}} - P_0}{P_0} \tag{5}$$

$P_{\mathrm{wb-max}}$ can be calculated by using equation (6) from Ref. [53].

$$P_{wb-max} = P_{\alpha-\mathrm{max}} + \frac{k_{r\alpha}}{q_\alpha \mu_\alpha}\rho_\alpha \cdot II \tag{6}$$

Where II is the injectivity index, calculated as

$$II = \frac{2\pi k dz}{\mathrm{In}(r_e/r_w) - 1/2} \tag{7}$$

$P_{\alpha-max}$ is the average of the maximum pressures in the injection grid cells of the two injection wells. The perforation layer thickness, dz, is 20 m, the well radius, r_w, is 0.07 m, and the grid block area is 100 m^2. q_α is the mass flowrate [kg/s], $k_{r\alpha}$ is the relative permeability [-], ρ_α and μ_α are the density [kg/m^3] and the dynamic viscosity [Pa.s] of the phase α, respectively.

(d) the average net geothermal electricity (measured in gigawatt-hours [GW_eh]) generated using the produced natural gas (via the organic/CO_2-based Rankine cycle) during the CNGR, Q_{CNGR}, and EGR,

Q_{EGR}, stages and from the produced CO_2 (via the direct CO_2 turbomachinery) during the direct-CPG stage, Q_{CPG}. The average net power generated is calculated using the output wellhead temperature and pressure results obtained from the wellbore heat transfer model described in Ref. [49]. The power system models applied in this study for the indirect and direct CO_2 turbomachinery power systems have also been extensively described in Ref. [40] and Ref. [49].

2.3 Parameter-space sensitivity analysis of the performance metrics

2.3.1 Residual methane content and CO_2-plume establishment stage

In our simulations, the residual CH_4 content is accounted for in the simulations using two main cases: Case 1 (base case) and Case 2, which consider the CNGR stage for 25 years and 26 years, respectively (Table 2). This implies that Case 2 has a lower residual CH_4 content than Case 1. Case 2 is equivalent to the example case presented in Ref. [49]. Case 2 is an example of a depleted reservoir, while Case 1 is an example of a partially depleted natural gas reservoir because it has a higher proportion of the residual CH_4 in the reservoir after the CNGR stage. These two cases are further classified into 4 sub-cases to represent cases with and without the 1.5 years of the CO_2-plume establishment (PE) stage. Cases 1-A and 2-A consider the 1.5 years of the PE stage, whereas Cases 1-B and 2-B do not consider the PE stage (Table 2). This enables us to investigate the effects of the PE stage on the production performance of the combined system in terms of ensuring annular flow in the production well, and in reducing the duration of the "expensive" transition period. The corresponding effects of these 4 sub-cases on the minimum CO_2 saturation in the well, natural gas recovery (during the CNGR and CO_2-EGR stages – including the transition period), the geothermal energy generation (during the 3 stages) performance metrics are also evaluated and discussed in this study (in Section 3.1).

Table 2: Description of the four cases used to show the effects of residual CH_4 content and CO_2-plume establishment stage on the performance metrics.

Cases	Case 1-A	Case 1-B	Case 2-A	Case 2-B
CNGR period (years)	25	25	26	26
Reservoir type	Partially depleted natural gas reservoir	Partially depleted natural gas reservoir	Depleted natural gas reservoir	Depleted natural gas reservoir
PE stage considered	Yes	No	Yes	No

2.3.2 Reservoir and operational parameters

Furthermore, we vary some key reservoir and operational (non-reservoir) parameters, in a fixed range of ±5% as compared to the base-case conditions (presented in Table 1) to investigate the sensitivity of the performance metrics of the combined system described in Section 2.2 to these parameters. The reservoir parameters (and their respective base-case values) that have been studied include, permeability (100 [mD]), anisotropy k_h/k_v (2.0 [-]), relative permeability (van Genuchten parameter of 0.77 [-]), and initial temperature (120 [°C]). The operational parameters (and their respective base-case values) that have been studied include well diameter (0.14 [m]) and average ambient surface temperature (15 [°C]). These base-case values correspond to the values chosen for the reservoir example presented in Ref. [49], except the reservoir initial temperature (150 °C was chosen in our previous study).

The simulations for each of the reservoir and operational parameter spaces considered in this study are run for a duration of 25 years for the CNGR stage and without considering the PE stage. The simulation results (high and low bounds) of the performance metrics for each of the respective parameter spaces are compared to the simulation results of the base-case example presented as Case 1-B (i.e. partially depleted natural gas reservoir without the PE stage).

The comparison indicates the sensitivity on the performance metrics (m) for a 5% change (both high and low) in the value of the parameter (X) from the base-case value considered in this study. Mathematically, we represent this sensitivity value, σ, as

$$\sigma = \frac{\left(m_{\text{high}} - m_{\text{low}}\right)/m_0}{\left(X_{\text{high}} - X_{\text{low}}\right)/X_0} \tag{8}$$

where m_0 and X_0 are the base-case performance metric result and the value of the parameter for the base case, respectively. The subscripts "high" and "low" denote the respective upper and lower bounds of the 5% deviation from the base-case value. We chose $\left(X_{\text{high}} - X_{\text{low}}\right)/X_0$ = 10% (i.e. 5% both ways from the base case). This implies that σ is a function of the performance metric results, m, and Equation (8) becomes

$$\sigma = 10 \cdot \frac{m_{\text{high}} - m_{\text{low}}}{m_0} \tag{9}$$

It should be noted that the non-reservoir (operational) parameters considered in this study do not affect the natural gas recovery performance and the pressure buildup metrics because these performance metrics are only dependent on the reservoir conditions. In addition, the sensitivity values obtained for the minimum CO_2 saturation in the well do not show any significant changes with the 5% deviation from the base case.

3. Results and discussions

3.1 Effects of residual CH_4 content and CO_2-plume establishment stage on the performance metrics

When the water saturation around the production well inlet is the highest, we consider whether the CO_2-plume establishment (PE) stage is required to ensure the desired [49] annular flow regime in the bottom-hole region of the production well. Recall that "A" denotes that the PE stage exists, whereas "B" denotes that the PE stage does not exist. Figure 2 shows that at the time of highest water saturation at the bottom-hole, Case 1-A has the highest CO_2 saturation in the reservoir and in the production well. This implies that the PE stage helps reduce the amount of water entering the production well. The results in Figure 3 show that the lower the residual CH_4 content after the CNGR stage, the higher the probability that the production well may experience slug/churn flow. However, for relatively low-diameter production wells (14 cm and 21 cm), the desired [49] annular flow is sustained even when the residual CH_4 content is very low (Cases 2-A and 2-B). As the production-well diameter increases to 33 cm, Case 2-B (depleted reservoir with no CO_2 plume establishment option) exhibits slug/churn flow at the bottom of the production well. Hence, if the diameter of the production well is relatively large, it may be necessary to include the CO_2 plume establishment (PE) stage. As discussed in Ref. [55], the optimal diameter of the production well needs to be determined not only to achieve an annular flow regime but also to maintain minimal pressure and heat losses in the production well.

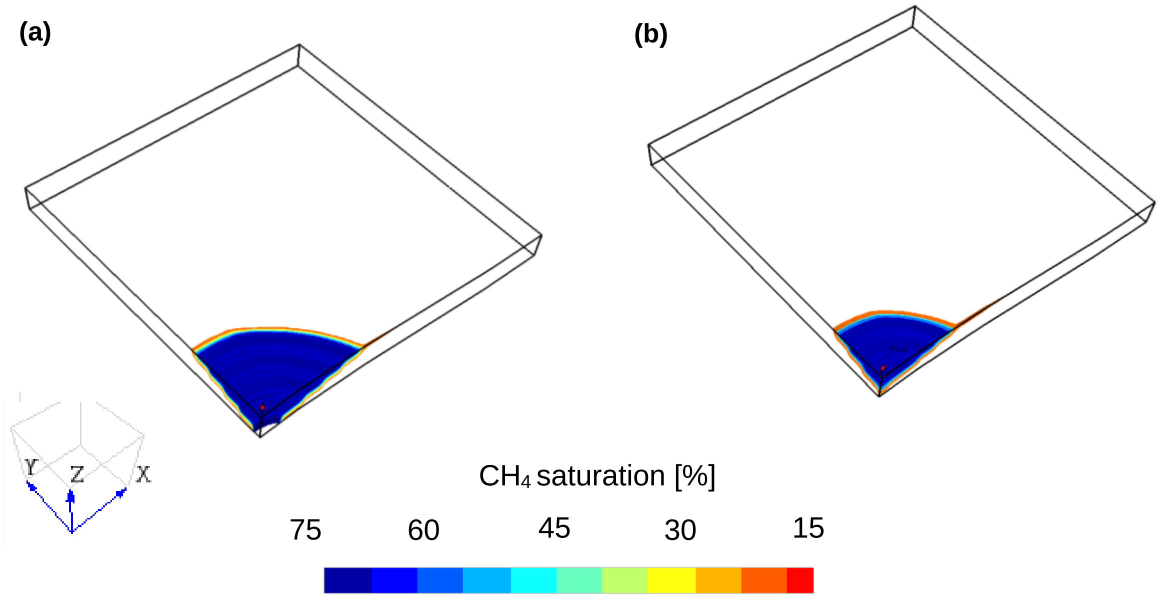

Figure 1: Quarter model showing the gas (ie. CH_4) saturation in the reservoir pore space after the CNGR stage for the partially depleted (a) and depleted (b) natural gas reservoir model. Note that the part of the models with CH_4 saturation less than 15% (i.e. high brine saturation) has been blanked.

We also investigate the effect of residual CH_4 content (in terms of partially depleted or depleted natural gas) on the natural gas recovery performance. The simulation results show that natural gas recovered during the CNGR is greater for the depleted reservoir scenario (see Table 3 and Figure A.1a in the Appendix). The natural gas recovery during the CO_2-EGR stage is higher for the cases without CO_2-plume establishment (Case 1-B and Case 2-B). This is because of the relatively high CO_2-CH_4 mixing rate that is associated with the CO_2-plume establishment stage, which may slightly reduce natural gas recovery during the CO_2-EGR+TP stage.

Table 3: Simulation results of the percentages of the original gas in place (OGIP) recovered during the CNGR and CO_2-EGR+TP stages, and associated natural gas recovery index (RI).

Cases	%OGIP recovered at CNGR stage	%OGIP recovered at EGR+TP stage	Total %OGIP recovered, F_{UR}	Duration of CO_2-EGR+TP stage (year)	Total duration of NG recovery (year)	RI (%/year)
Case 1-A: 25 years w/PE	83.51	3.48	86.99	1.50	28.50	3.28
Case 1-B: 25 years no PE	83.51	7.43	90.94	3.82	28.82	3.16
Case 2-A: 26 years w/PE	86.85	0.63	87.48	2.00	28.00	3.12
Case 2-B: 26 years no PE	86.85	2.84	89.69	2.97	28.97	3.10

From Table 3, we observe a decrease in the number of years for the expensive separation period in the CO_2-EGR+TP stage for the two cases that consider the PE stage, which leads to a higher recovery index (RI). For the partially depleted NG reservoir example cases, the expensive separation duration reduces when the PE stage is considered (i.e. Case 1-A), and this leads to better performance (higher RI) for Case 1-A than for Case 1-B. Table 3 also shows that the calculated RI is lower for the depleted NG reservoir example cases, and there is only a slight increase in RI between Cases 2-A and 2-B. Hence, the simulation results show that the effect of the PE stage on the natural gas recovery index is more pronounced when the reservoir is partially depleted of natural gas. However, if the natural gas reservoir is depleted, the PE stage is important to establish a CO_2 connection between the injectors and producers.

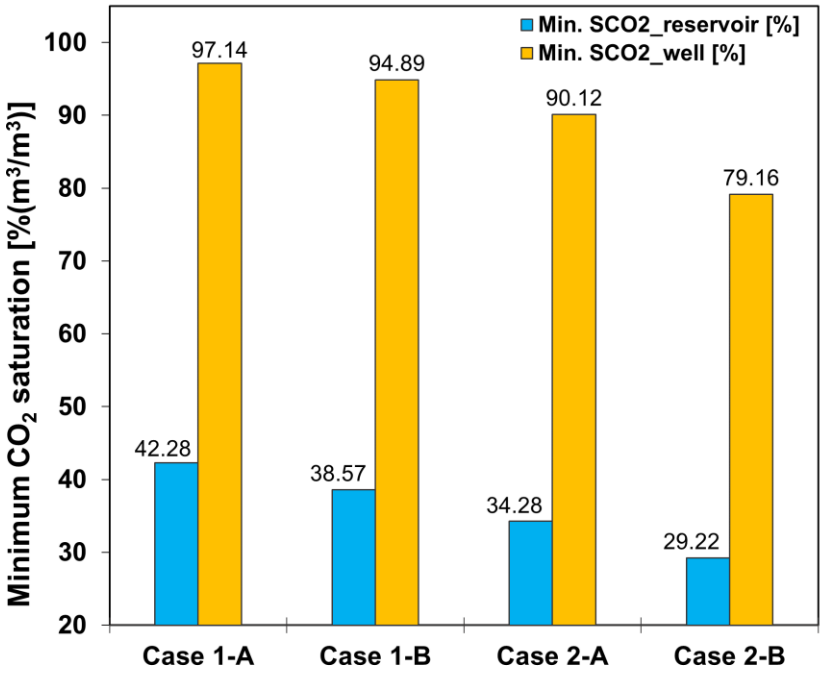

Figure 2: Simulation results, for partially depleted (Case 1) and depleted (Case 2) natural gas reservoirs, representing different residual CH_4 content with (A) and without (B) including the CO_2-plume establishment (PE) stage, showing the minimum gas (i.e. mainly CO_2) saturation in the reservoir pore space immediately surrounding the production well inlet (blue bars) and inside the production well (bottomhole) itself (yellow bars). These results imply that the amount of water in the bottomhole of the production well is 2.86% vol. (Case 1-A), 5.11% vol. (Case 1-B), 9.88% vol. (Case 2-A), and 20.84% vol. (Case 2.-B).

During the CNGR stage, more geothermal energy is generated from the natural gas for the depleted reservoir cases (Case 2) than the partially depleted reservoir cases (Case 1), as shown in Table 4 and Figure A.2, as the amount of natural gas recovered from the depleted NG reservoir is greater than that recovered from the partially depleted NG reservoir. The opposite is the case for the CO_2-EGR+TP stage during which more NG, and hence more associated geothermal energy, is produced from the partially depleted reservoir (see Table 3). During the CPG stage, Case 1-A has the highest value of geothermal electricity generated (Table 4). This is because it has the shortest duration of the CO_2-EGR+TP stage (1.50 years), which ensures an earlier start, and longer duration, of the CPG stage.

Of all four cases considered, the combined CO_2-EGR–CPG system in a partially depleted NG reservoir which includes a PE stage (Case 1-A) yields the best results in terms of: (i) the desired [49] annular flow regime in the production well, (ii) the natural gas recovery performance (including having the shortest duration of the CO_2-EGR+TP stage), and (iii) the average total net electricity generation performance. Hence, it appears advantageous to plan the combined CO_2-EGR–CPG system (including the PE stage) to commence before the natural gas reservoir is completely depleted.

Preprints (www.preprints.org) | NOT PEER-REVIEWED | Posted: 13 September 2021 doi:10.20944/preprints202109.0203.v1

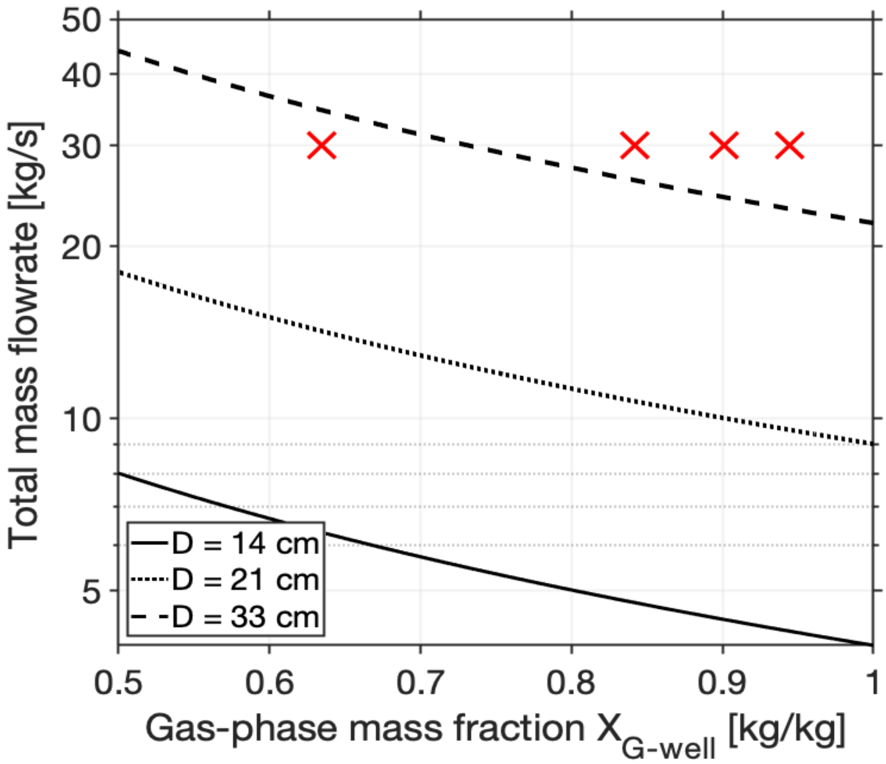

Figure 3: Two-phase wellbore flow regime plot showing the total mass flowrate of all fluids [kg/s] over the gas-phase mass fraction [kg/kg] at the bottom of the well defined as $X_{G-well} = \frac{S_{\mathrm{G-well}} \cdot \varrho_G}{S_{\mathrm{L-well}} \cdot \varrho_L + S_{\mathrm{G-well}} \cdot \varrho_G}$, where $S_{\mathrm{G-well}}$ is the gas-phase saturation in the well, $S_{\mathrm{L-well}}$ is the water-phase saturation in the well, and ϱ denotes density. The plotted symbols show the lowest gas-phase mass fraction points of the four investigated cases (Table 2) for three production well diameters, *D*. The lines indicate the minimum flow rate required to achieve the desired annular flow regime in the production well. Hence, conditions above each line indicate the annular flow regime, while conditions below each line indicate the undesired slug/churn flow regime in the production well.

Table 4: Simulation results for the net geothermal electricity generation performance metrics during the four stages of the combined CO_2-EGR–CPG system, calculated for the four cases (considering residual methane content and the PE stage).

Cases	**Net electricity generated at CNGR stage [GW$_e$h]**	**Net electricity generated at CO_2-EGR+TP stage [GW$_e$h]***	**Net electricity generated at CPG stage [GW$_e$h]****	**Total net electricity generated during the project [GW$_e$h]**
Case 1-A: 25 years w/ PE	9.163	0.676	232.048	241.887
Case 1-B: 25 years no PE	9.163	1.767	173.443	184.373
Case 2-A: 26 years w/ PE	9.246	0.484	214.514	224.244
Case 2-B: 26 years no PE	9.246	0.599	199.342	209.184

* The duration of the respective CO_2-EGR+TP stage, for each of the 4 cases, is given in Table 3.
** The duration of the respective CPG stage, for each of the 4 cases, is calculated as the end year – the durations of the CNGR and CO_2-EGR+TP stages.

3.2 Effects of reservoir and operational parameters on the performance metrics

3.2.1 Natural gas recovery performance and maximum fluid pressure buildup

Recall that the natural gas recovery performance (NGRP) metric is only dependent on the changes in the reservoir parameters and not on non-reservoir parameters. As described in Section 2.2, the NGRP is determined in this study by the value of the natural gas recovery index (RI), which can be calculated using Equation (4). Figure A.1b-e show the volume of natural gas recovered (in %OGIP) during the CNGR and CO_2-EGR stages for the different reservoir parameters considered in this study. Figure 4 shows the sensitivity for the reservoir parameters considered in this study on the natural gas recovery performance for the CNGR and the CO_2-EGR+TP stages (when natural gas is being produced and methane is separated from CO_2). The parameters plotted on the upper part of the horizontal logarithmic axis (Figure 4) indicate those with a positive sensitivity value (σ), and those parameters that are plotted on the lower part of the axis have a negative σ. A positive (+) value of σ shows that there is an increase in the NGRP when the value of the parameter increases, whereas the opposite is the case for a negative (–) value of σ.

The sensitivity results, plotted in Figure 4, show that permeability anisotropy and reservoir temperature are the most sensitive parameters (both ~ 0.2) to the NGRP, with each having a different sign of the sensitivity value. We observe that, as the permeability anisotropy increases, the NGRP significantly decreases (i.e. negative σ value). This is the case as the production well is perforated only over the topmost layer interval (20 m out of the entire 100 m reservoir thickness), and a decrease in the vertical permeability (i.e. increase in permeability anisotropy) leads to less upward flow of the natural gas towards the production-well perforation. Hence, the decrease in NGRP. However, an increase in reservoir temperature would lead to a significant increase in the NGRP, as the kinematic viscosity of the gas is reduced at higher temperatures, increasing the gas mobility. The horizontal permeability parameter is the least sensitive parameter for the NGRP, with a sensitivity value of +0.0045, which is two orders of magnitude less than those of the most sensitive parameters.

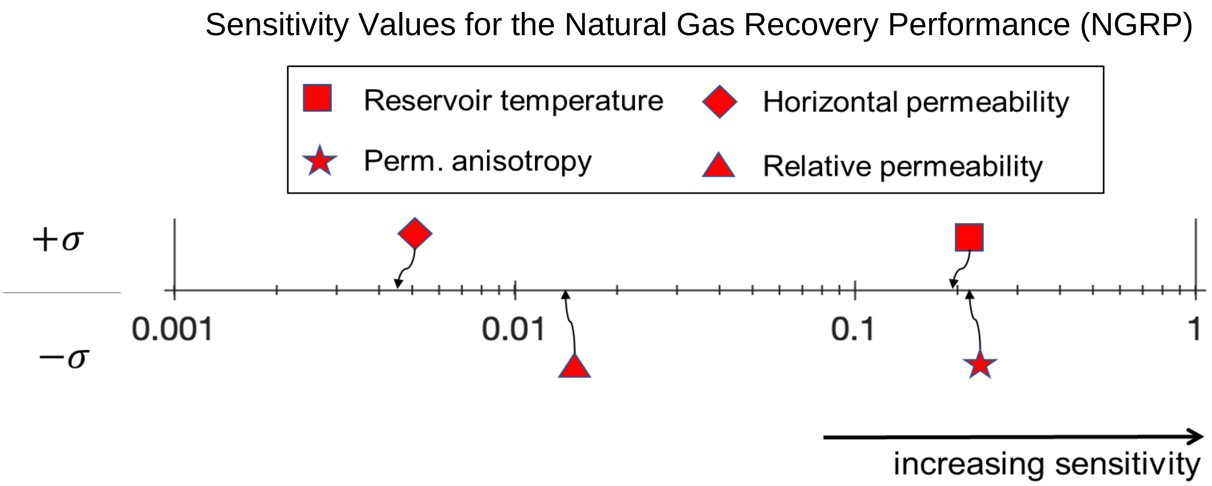

Figure 4: Sensitivity values (plotted on a logarithmic axis) for the natural gas recovery performance (NGRP) metric for the reservoir parameters considered in this study for the CNGR and the CO_2-EGR+TP stages. This is only calculated during the CNGR and CO_2-EGR+TP stages. The positive (upper) part signifies that an increase in the parameter values will improve the NGRP. The negative (lower) part identifies parameters that, when being increased, will result in a decrease in the NGRP.

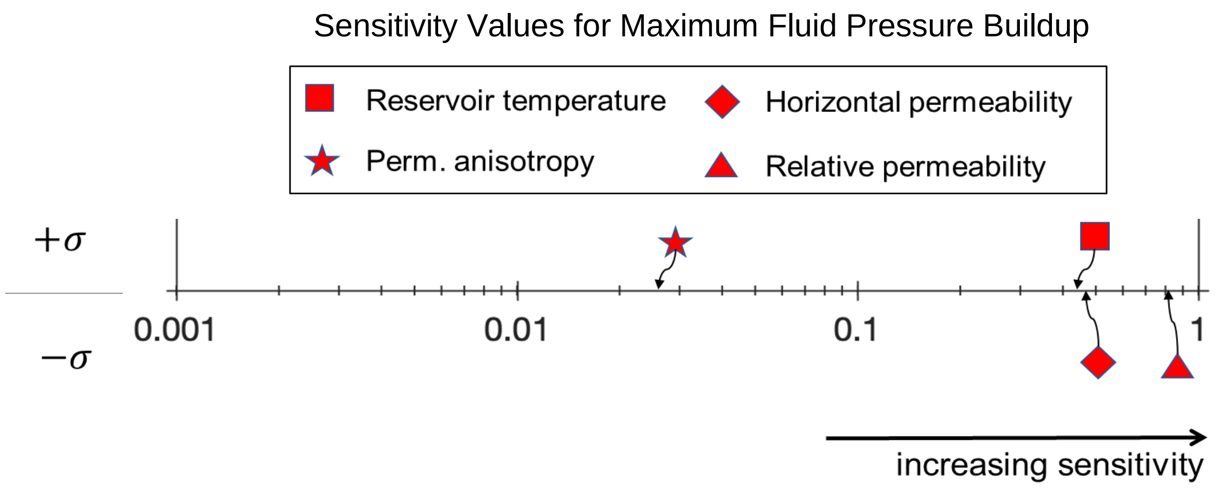

Figure 5: Sensitivity values (plotted on a logarithmic axis) for the fluid pressure buildup metric for the reservoir parameters considered in this study. The positive (upper) part signifies that an increase in the parameter values will increase the fluid pressure buildup. The negative (lower) part identifies parameters that, when being increased, will result in a decrease in the fluid pressure buildup.

The sensitivity results for the maximum fluid pressure buildup, plotted in Figure 5, show that the van Genuchten relative permeability is the most sensitive parameter, followed by horizontal permeability and reservoir temperature. The sensitivity to the van Genuchten relative permeability is because the maximum fluid pressure buildup happens during the CO_2-EGR+TP stage when two-phase flow processes near the injection wells are important. An increase in horizontal permeability leads to a decrease in pressure buildup intensity, hence a high (negative) sensitivity value is observed for this parameter. The sensitivity to reservoir temperature is a result of the constant CO_2 injection mass flow rate used. If a constant volume flowrate were applied instead, the fluid pressure buildup would be significantly less sensitive to reservoir temperature. Figure 5 also shows that the fluid pressure buildup metric is not sensitive to permeability anisotropy changes.

3.2.2 Geothermal energy (electricity) generation performance during the CNGR, CO_2-EGR+TP and CPG stages

During the CNGR stage, the average net power and electricity generated by the base-case example (i.e. Case 1-B, described in Section 3.1) are 0.042 MW_e and 9.16 GW_eh over 25 years. The time series plots of the simulation results, showing the net power generated for the different parameters considered in this study, can be found in the Appendix (Figure A.3 to Figure A.8). Figure 6 shows that the most sensitive parameter that influences the net electrical geothermal energy generated during the CNGR stage is the reservoir temperature (σ = +5.0), followed by the mean surface ambient temperature (σ = –0.5). It is no surprise that the net energy generated increases with an increase in reservoir temperature but decreases with an increase in the mean surface ambient temperature. The permeability anisotropy parameter is the least sensitive parameter for this performance metric during the CNGR stage. The sensitivity value (–0.0015) for the permeability anisotropy differs by 3 orders of magnitude from that of the reservoir temperature parameter. Figure 6 also shows that during the CNGR stage, changes in the other parameters considered in this study have little effect on the geothermal energy generation performance, with their sensitivity values of $\sigma < \pm0.1$.

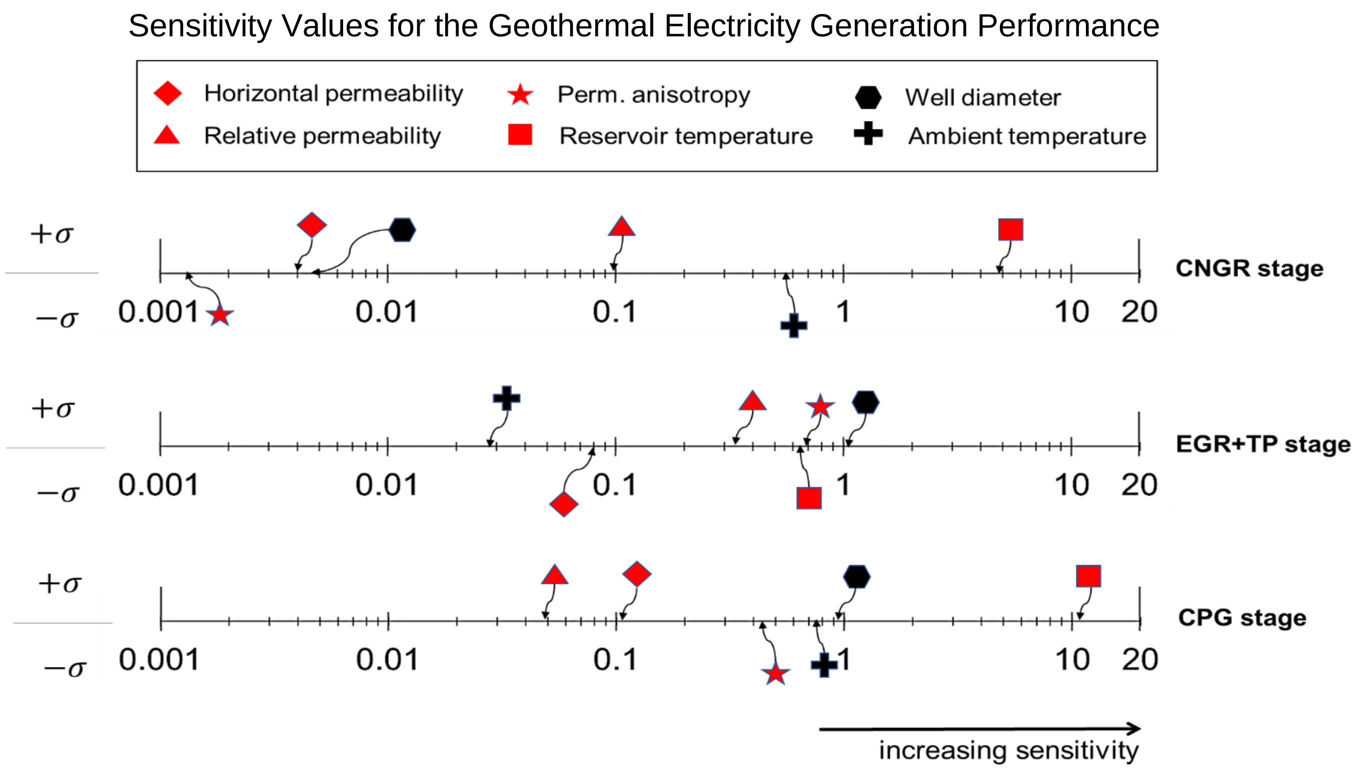

Figure 6: Sensitivity values (plotted on a logarithmic axis) for the geothermal electricity generation performance metric for the reservoir and operational parameters considered in this study. This is calculated for the three main stages of the combined system. The positive (upper) part signifies that an increase in the parameter values will increase the geothermal power output. The negative (lower) part identifies parameters that, when being increased, will result in a decrease in the geothermal power output.

During the CO_2-EGR+TP stage, the average net power and the electricity generated for the base-case example are 0.053 MW_e and 1.78 GW_eh (over 3.82 years). From Figure 6, we observe that the most sensitive parameter for the CO_2-EGR+TP stage is the production wellbore diameter, with σ = +1.50. This is because during this stage, the CO_2 mass fraction increases, leading to a higher density of the fluid flowing in the well and causing higher pressure losses due to friction as the well diameter decreases. This reduces the amount of energy extractable from the produced/separated methane. The least sensitive parameter is the mean ambient surface temperature, with σ = +0.028. In Figure 4, we showed that the reservoir temperature has a high influence on NGRP, and here (Figure 6) we also see that the reservoir temperature is the third most sensitive parameter for the energy generation performance during the CO_2-EGR+TP stage. This is because the energy generated during the CO_2-EGR+TP stage is proportional to the volume of natural gas produced and the duration of the CO_2-EGR+TP stage.

During the CPG stage (when the CO_2 mass fraction is >90% and only the direct CO_2-thermosiphon power system model is used), the average net power and the geothermal energy generated for the base case example are 0.739 MW_e and 173.44 GW_eh (over 27.18 years). This is about 14.0 –17.5 times higher than the average net power generated during the CNGR and CO_2-EGR+TP stages, respectively. This is due to the use of the direct CPG power system [40] and the increase in production mass flowrate from 4 kg/s to 30 kg/s applied during this stage. Note that the energy generated by the other cases (Cases 1-A, 2-A, and 2-B) considered in this study (in Section 3.1) is greater than the base case (Case 1-B) used for the parameter space sensitivity study.

As expected, the most sensitive parameter for this CPG stage is reservoir temperature, with a sensitivity value of σ > +10.0 (Figure 6). The wellbore diameter and the mean surface ambient temperature also show high sensitivity values, during the CPG stage, because, as the wellbore diameter increases, the fluid pressure and the heat losses decrease, while lower mean surface ambient temperatures favor higher net energy extraction and power generation rates at the land surface. The least sensitive parameter during this CPG stage is the relative permeability with a σ that is more than 2 orders of magnitude lower than that for the reservoir temperature. This is caused by a constant CO_2 flow rate in this study. If instead the fluid pressure difference between the injection and the production wells were kept constant, permeability would be a key parameter.

In this study, we can observe that reservoir temperature is the most important parameter for the combined CO_2-EGR–CPG system, especially during the CNGR and CPG stages. The second most important parameter is the production wellbore diameter, which can be adjusted, i.e. engineered. Interestingly, the performance metrics, except for pressure buildup, studied here are not particularly sensitive to the van Genuchten relative-permeability parameter for pore-size distribution.

4. Conclusions

We have presented a reservoir simulation study to investigate the effects of residual CH_4 content and the CO_2-plume establishment (PE) stage on achieving an annular flow regime in the production well, when a specified mass flow rate is used in a combined CO_2 enhanced gas recovery (EGR) – CO_2 plume geothermal (CPG) system. In addition, the effects of residual CH_4 content and PE-stage existence, including the sensitivity of some key reservoir and operational parameters, on the natural gas recovery and geothermal energy generation performances of the combined CO_2-EGR–CPG system have been investigated. Our key results and findings are:

1. The simulation results show that the PE stage is important to establish the desired annular flow regime near the bottom of the production well, especially when large-diameter wells are used. However, it is possible to achieve an annular flow regime by using wells with smaller diameters.

2. The simulation results show that commencing with the injection of CO_2 into the natural gas reservoir before it is completely depleted and including the CO_2-plume establishment stage increase the natural gas recovery performance over the entire project duration. This is due to the high recovery index (relatively high ultimate recovery factor and the shortest duration of the CO_2-CH_4 separation period) associated with this implementation of the combined CO_2-EGR–CPG system.

3. The simulation results also show that out of the four reservoir parameters (permeability anisotropy, horizontal permeability, relative permeability, and reservoir temperature) considered in this study, permeability anisotropy and reservoir temperature are the parameters that most strongly influence the natural gas recovery performance (NGRP) of the combined CO_2-EGR–CPG system. The simulation results also show that the fluid pressure buildup at the injection wells is most sensitive to changes in the van Genuchten relative permeability and horizontal-permeability parameters.

4. A shorter duration of the CO_2-EGR+TP stage is achieved when a PE stage is included. The PE stage serves as an important transitional stage for later CPG operations, due to the quick increase in the CO_2 saturation in the reservoir pore space and fast establishment of a CO_2 connection between the injection and the production wells.

5. The sensitivity results reveal that for a given CO_2 flowrate, the reservoir temperature is the parameter the geothermal power generation performance is most sensitive to. The production wellbore diameter is the second-most sensitive parameter. Changes in the van Genuchten relative permeability parameter for pore-size distribution do not have a significant influence on the geothermal power generation performance of the combined CO_2-EGR–CPG system.

Acknowledgment

The authors would like to thank the State Secretariat for Education, Research and Innovation (SERI), Switzerland, for a Swiss Government Excellence Scholarships for Foreign Scholars and Artists that supported this study. The Werner Siemens Foundation (Werner Siemens-Stiftung) is also thanked by Martin O. Saar for its support of the Geothermal Energy and Geofluids (GEG.ethz.ch) Group at ETH Zurich, Switzerland.

Conflicts of Interest: The authors declare no conflict of interest.

References

1. Bert, M.; Davidson, O.; Coninck, H. de; Loos, M.; Meyer, L. *IPCC special report on carbon dioxide capture and storage*; 2005;
2. Global CCS Institute *Global status of CCS: Targeting climate change*; 2019;
3. Townsend, A.; Raji, N.; Zapantis, A. *The value of carbon capture and storage (CCS)*; 2020;
4. International Energy Agency World Energy Outlook 2018. **2018**, 661, doi:10.1787/weo-2018-2-en.
5. Oldenburg, C.M.; Pruess, K.; Benson, S.M. Process modeling of CO_2 injection into natural gas reservoirs for carbon sequestration and enhanced gas recovery. *Energy & Fuels* **2001**, *15*, 293–298, doi:Doi 10.1021/Ef000247h.
6. Oldenburg, C..; Stevens, S..; Benson, S.. Economic feasibility of carbon sequestration with enhanced gas recovery (CSEGR). *Energy* **2004**, *29*, 1413–1422, doi:https://doi.org/10.1016/j.energy.2004.03.075.
7. Polak, S.; Grimstad, A.A. Reservoir simulation study of CO_2 storage and CO_2-EGR in the Atzbach–Schwanenstadt gas field in Austria. In Proceedings of the Energy Procedia; 2009; Vol. 1, pp. 2961–2968.
8. Leeuwenburgh, O.; Neele, F.; Hofstee, C.; Weijermans, P.-J.; de Boer, H.; Oosthoek, P.; Lefebvre, A.; Godderij, R.; Gutierrez-Neri, M. Enhanced Gas Recovery – a Potential 'U' for CCUS in The Netherlands. In Proceedings of the Energy Procedia; Elsevier, 2014; Vol. 63, pp. 7809–7820.
9. Koide, H.; Tazaki, Y.; Noguchi, Y.; Iijima, M.; Ito, K.; Shindo, Y. Underground storage of carbon dioxide in depleted natural gas reservoirs and in useless aquifers. *Eng. Geol.* **1993**, *34*, 175–179, doi:10.1016/0013-7952(93)90086-R.
10. van der Burgt, M.J.; Cantle, J.; Boutkan, V.K. Carbon dioxide disposal from coal-based IGCC's in depleted gas fields. *Energy Convers. Manag.* **1992**, *33*, 603–610, doi:10.1016/0196-8904(92)90062-2.
11. Papay, J. Improved recovery of conventional natural gas. Part I: Theortical discussion of recovery methods. *Erdoel, Erdgas, Kohle* **1999**, *6*, 302–308.

12. Papay, J. Improved recovery of conventional natural gas. Part II: Results of a pilot test. *Erdoel Erdgas Kohle* **1999**, *115*, 354–356.
13. Van Der Meer, L.G.; Kreft, E.; Geel, C.; Hartman, J. K12-B A Test site for CO_2 storage and enhanced gas recovery. In Proceedings of the SPE Europec/EAGE Annual Conference and Exhibition, Madrid, Spain, 13-16 June; 2005; pp. 1–9.
14. Van Der Meer, B.L.G.H.; Arts, R.J.; Geel, C.R.; Hofstee, C.; Winthaegen, P.; Hartman, J.; D'Hoore, D. K12-B: Carbon Dioxide Injection in a Nearly Depleted Gas Field Offshore the Netherlands. In Proceedings of the Carbon Dioxide Sequestration in Geological Media—State of the Science; Grobe, M., Pashin, J.C., Dodge, R.L., Eds.; American Association of Petroleum Geologists, 2009; Vol. 59, p. 0.
15. Denney, D. Technical and economic challenge of mature gas fields: The Giant Altmark Field, Germany. *J. Pet. Technol.* **2006**, *58*, 38–39, doi:10.2118/0106-0038-JPT.
16. Kühn, M.; Förster, A.; Großmann, J.; Meyer, R.; Reinicke, K.; Schäfer, D.; Wendel, H. CLEAN: Preparing for a CO_2-based enhanced gas recovery in a depleted gas field in Germany. In Proceedings of the Energy Procedia; Elsevier, 2011; Vol. 4, pp. 5520–5526.
17. Kühn, M.; Tesmer, M.; Pilz, P.; Meyer, R.; Reinicke, K.; Förster, A.; Kolditz, O.; Schäfer, D.; CLEAN Partners CLEAN: project overview on CO_2 large-scale enhanced gas recovery in the Altmark natural gas field (Germany). *Environ. Earth Sci.* **2012**, *67*, 311–321, doi:10.1007/s12665-012-1714-z.
18. Oldenburg, C.M.; Benson, S.M. CO_2 injection for enhanced gas production and carbon sequestration. In Proceedings of the SPE International Petroleum Conference and Exhibition in Mexico; Society of Petroleum Engineers: Villahermosa, Mexico, 2002; pp. 1–10.
19. Oldenburg, C.M. Carbon dioxide as cushion gas for natural gas storage. *Energy & Fuels* **2003**, *17*, 240–246, doi:10.1021/ef020162b.
20. Jikich, S.A.; Smith, D.H.; Sams, W.N.; Bromhal, G.S. Enhanced gas recovery (EGR) with carbon dioxide sequestration: A simulation study of effects of injection strategy and operational parameters. In Proceedings of the SPE Eastern Regional Meeting; Society of Petroleum Engineers: Pittsburgh, Pennsylvania, 2003; pp. 1–9.
21. Rückheim, J.; Voigtlaender, G.; Stein-Khokhlov, M. The technical and economic challenge of "mature gas fields": The Giant Altmark Field, a German example. In Proceedings of the SPE Europec/EAGE Annual Conference; Society of Petroleum Engineers: Madrid, Spain, 2005; pp. 1–4.
22. Gou, Y.; Hou, Z.; Liu, H.; Zhou, L.; Were, P. Numerical simulation of carbon dioxide injection for enhanced gas recovery (CO_2-EGR) in Altmark natural gas field. *Acta Geotech.* **2014**, *9*, 49–58, doi:10.1007/s11440-013-0221-z.
23. Procesi, M.; Cantucci, B.; Buttinelli, M.; Armezzani, G.; Quattrocchi, F.; Boschi, E. Strategic use of the underground in an energy mix plan: Synergies among CO_2, methane geological storage and geothermal energy. Latium Region case study (Central Italy). *Appl. Energy* **2013**, *110*, 104–131, doi:10.1016/J.APENERGY.2013.03.071.
24. Clemens, T.; Secklehner, S.; Mantatzis, K.; Jacobs, B. Enhanced gas recovery, challenges shown at the example of three gas fields. In Proceedings of the SPE EUROPEC/EAGE Annual Conference and Exhibition held in Barcelona, Spain, 14– 17 June; 2010; pp. 1–17.
25. Polak, S.; Zweigel, J.; Lindeberg, E.; Pannetier-Lescoffit, S.; Schulz, H.-M.; Faber, E.; Teschner, M.; Poggenburg, J.; May, F.; Krooss, B.; et al. The Atzbach-Schwanenstadt gas field - A potential site for onshore CO_2 storage and EGR. *Geophysics* **2006**, *25*.
26. Khan, C.; Amin, R.; Madden, G. Carbon dioxide injection for enhanced gas recovery and storage (reservoir simulation). *Egypt. J. Pet.* **2013**, *22*, 225–240, doi:10.1016/j.ejpe.2013.06.002.
27. Regan, M.L.M. A Numerical Investigation into the Potential to Enhance Natural Gas Recovery in

Water-drive Gas Reservoirs through the Injection of CO_2, The University of Adelaide, 2010.

28. Xie, H.; Li, X.; Fang, Z.; Wang, Y.; Li, Q.; Shi, L.; Bai, B.; Wei, N.; Hou, Z. Carbon geological utilization and storage in China: current status and perspectives. *Acta Geotech.* **2014**, *9*, 7–27, doi:10.1007/s11440-013-0277-9.

29. Shi, Y.; Jia, Y.; Pan, W.; Huang, L.; Yan, J.; Zheng, R. Potential evaluation on CO_2-EGR in tight and low-permeability reservoirs. *Nat. Gas Ind. B* **2017**, *4*, 311–318, doi:10.1016/J.NGIB.2017.08.013.

30. Dutcher, B.; Fan, M.; Russell, A.G. Amine-based CO_2 capture technology development from the beginning of 2013 — A review. *ACS Appl. Mater. Interfaces* **2015**, *7*, 2137–2148, doi:10.1021/am507465f.

31. Brunetti, A.; Scura, F.; Barbieri, G.; Drioli, E. Membrane technologies for CO_2 separation. *J. Memb. Sci.* **2010**, *359*, 115–125, doi:https://doi.org/10.1016/j.memsci.2009.11.040.

32. Rybach, L. Geothermal energy: sustainability and the environment. *Geothermics* **2003**, *32*, 463–470, doi:10.1016/S0375-6505(03)00057-9.

33. Axelsson, G.; Stefánsson, V.; Björnsson, G.; Liu, J. Sustainable management of geothermal resources and utilization for 100-300 years. In Proceedings of the Proceedings World Geothermal Congress, International Geothermal Association, Antalya, Turkey, 24-29 April; 2005; pp. 1–8.

34. Lund, J.W.; Boyd, T.L. Direct utilization of geothermal energy 2015 worldwide review. *Geothermics* **2016**, *60*, 66–93, doi:10.1016/J.GEOTHERMICS.2015.11.004.

35. Brown, D.W. A hot dry rock geothermal energy concept utilizing supercritical CO_2 instead of water. In Proceedings of the Proceedings of the Twenty-Fifth Workshop on Geothermal Reservoir Engineering; Stanford, California, 2000; pp. 1–6.

36. Pruess, K. Enhanced Geothermal Systems (EGS) comparing water with CO_2 as heat transmission fluids. In Proceedings of the New Zealand Geothermal Workshop; University of Auckland, Auckland, New Zealand., 2007; pp. 1–13.

37. Pruess, K. Enhanced geothermal systems (EGS) using CO_2 as working fluid-A novel approach for generating renewable energy with simultaneous sequestration of carbon. *Geothermics* **2006**, *35*, 351–367, doi:10.1016/j.geothermics.2006.08.002.

38. Randolph, J.B.; Saar, M.O. Combining geothermal energy capture with geologic carbon dioxide sequestration. *Geophys. Res. Lett.* **2011**, *38*, 1–7, doi:10.1029/2011GL047265.

39. Adams, B.M.; Kuehn, T.H.; Bielicki, J.M.; Randolph, J.B.; Saar, M.O. On the importance of the thermosiphon effect in CPG (CO_2 plume geothermal) power systems. *Energy* **2014**, *69*, 409–418, doi:10.1016/j.energy.2014.03.032.

40. Adams, B.M.; Kuehn, T.H.; Bielicki, J.M.; Randolph, J.B.; Saar, M.O. A comparison of electric power output of CO_2 Plume Geothermal (CPG) and brine geothermal systems for varying reservoir conditions. *Appl. Energy* **2015**, *140*, 365–377, doi:10.1016/J.APENERGY.2014.11.043.

41. Atrens, A.; Gurgenci, H.; Rudolph, V. Exergy analysis of a CO_2 thermosiphon. In Proceedings of the Proceedings of the Thirty-Fourth Workshop on Geothermal Reservoir Engineering; Stanford, California, 2009; pp. 1–6.

42. Pruess, K. On production behavior of enhanced geothermal systems with CO_2 as working fluid. *Energy Convers. Manag.* **2008**, *49*, 1446–1454, doi:https://doi.org/10.1016/j.enconman.2007.12.029.

43. Wang, C.L.; Cheng, W.L.; Nian, Y. Le; Yang, L.; Han, B.B.; Liu, M.H. Simulation of heat extraction from CO_2-based enhanced geothermal systems considering CO_2 sequestration. *Energy* **2018**, *142*, doi:10.1016/j.energy.2017.09.139.

44. Majer, E.L.; Baria, R.; Stark, M.; Oates, S.; Bommer, J.; Smith, B.; Asanuma, H. Induced seismicity associated with Enhanced Geothermal Systems. *Geothermics* **2007**, *36*, 185–222,

doi:https://doi.org/10.1016/j.geothermics.2007.03.003.

45. Amann, F.; Gischig, V.; Evans, K.; Doetsch, J.; Jalali, R.; Valley, B.; Krietsch, H.; Dutler, N.; Villiger, L.; Brixel, B.; et al. The seismo-hydromechanical behavior during deep geothermal reservoir stimulations: open questions tackled in a decameter-scale in situ stimulation experiment. *Solid Earth* **2018**, *9*, 115–137, doi:10.5194/se-9-115-2018.
46. Randolph, J.B.; Saar, M.O. Coupling carbon dioxide sequestration with geothermal energy capture in naturally permeable, porous geologic formations: Implications for CO_2 sequestration. In Proceedings of the Energy Procedia; Elsevier, 2011; Vol. 4, pp. 2206–2213.
47. Garapati, N.; Randolph, J.B.; Saar, M.O. Brine displacement by CO_2, energy extraction rates, and lifespan of a CO_2-limited CO_2-Plume Geothermal (CPG) system with a horizontal production well. *Geothermics* **2015**, *55*, 182–194, doi:10.1016/j.geothermics.2015.02.005.
48. Adams, B.M.; Vogler, D.; Kuehn, T.H.; Bielicki, J.M.; Garapati, N.; Saar, M.O. Heat Depletion in Sedimentary Basins and its Effect on the Design and Electric Power Output of CO2 Plume Geothermal (CPG) Systems. *Renew. Energy* **2021**, *172*, 1393–1403, doi:https://doi.org/10.1016/j.renene.2020.11.145.
49. Ezekiel, J.; Ebigbo, A.; Adams, B.M.; Saar, M.O. Combining natural gas recovery and CO_2-based geothermal energy extraction for electric power generation. *Appl. Energy* **2020**, *269*, 1–21, doi:https://doi.org/10.1016/j.apenergy.2020.115012.
50. Hefny, M.; Qin, C.; Saar, M.O.; Ebigbo, A. Synchrotron-based pore-network modeling of two-phase flow in Nubian Sandstone and implications for capillary trapping of carbon dioxide. *Int. J. Greenh. Gas Control* **2020**, *103*, 103164, doi:https://doi.org/10.1016/j.ijggc.2020.103164.
51. Fleming, M.R.; Adams, B.M.; Kuehn, T.H.; Bielicki, J.M.; Saar, M.O. Increased Power Generation due to Exothermic Water Exsolution in CO_2 Plume Geothermal (CPG) Power Plants. *Geothermics* **2020**, *88*, 101865, doi:https://doi.org/10.1016/j.geothermics.2020.101865.
52. Zhang, L.; Li, X.; Zhang, Y.; Cui, G.; Tan, C.; Ren, S. CO_2 injection for geothermal development associated with EGR and geological storage in depleted high-temperature gas reservoirs. *Energy* **2017**, *123*, 139–148, doi:10.1016/j.energy.2017.01.135.
53. Pruess, K.; Oldenburg, C.; Moridis, G. *TOUGH2 user's guide, version 2 (revised)*; 2012;
54. Oldenburg, C.M.; Moridis, G.J.; Spycher, N.; Pruess, K. *EOS7C Version 1.0: TOUGH2 Module for cambon dioxide or nitrogen in natural gas (methane) reservoirs*; 2004;
55. Ezekiel, J.; Adams, B.M.; Saar, M.O.; Ebigbo, A. Numerical analysis and optimization of the performance of CO2-plume geothermal (CPG) production wells and implications for electric power generation (under review). *Geothermics* **2021**.

Preprints (www.preprints.org) | NOT PEER-REVIEWED | Posted: 13 September 2021 doi:10.20944/preprints202109.0203.v1

Appendix

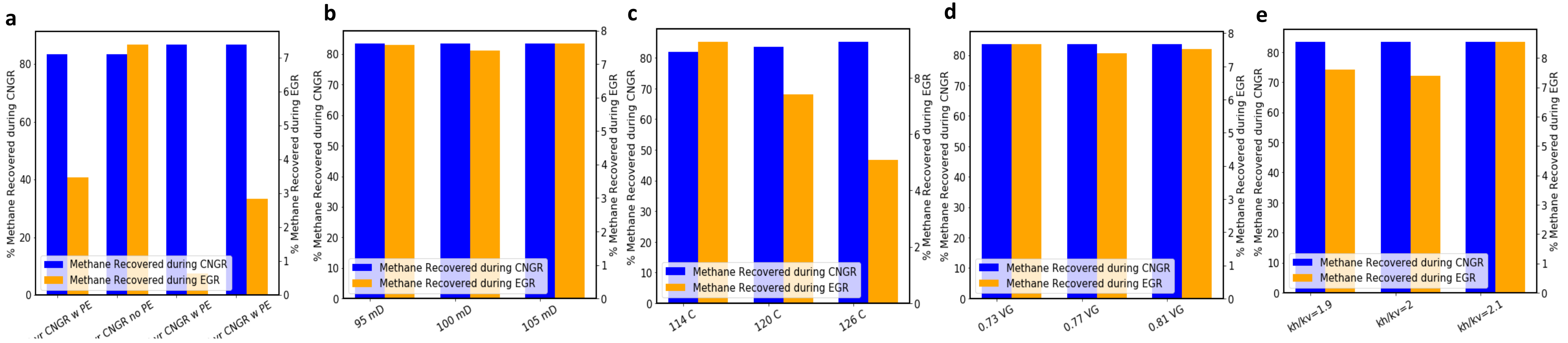

Figure A.1: Percentage of original gas in place (OGIP) recovered during the CNGR and EGR stages for the 4 reservoir model example cases (a) and the 4 reservoir parameters [permeability (b), temperature (c), relative permeability (d), and permeability anisotropy (e)].

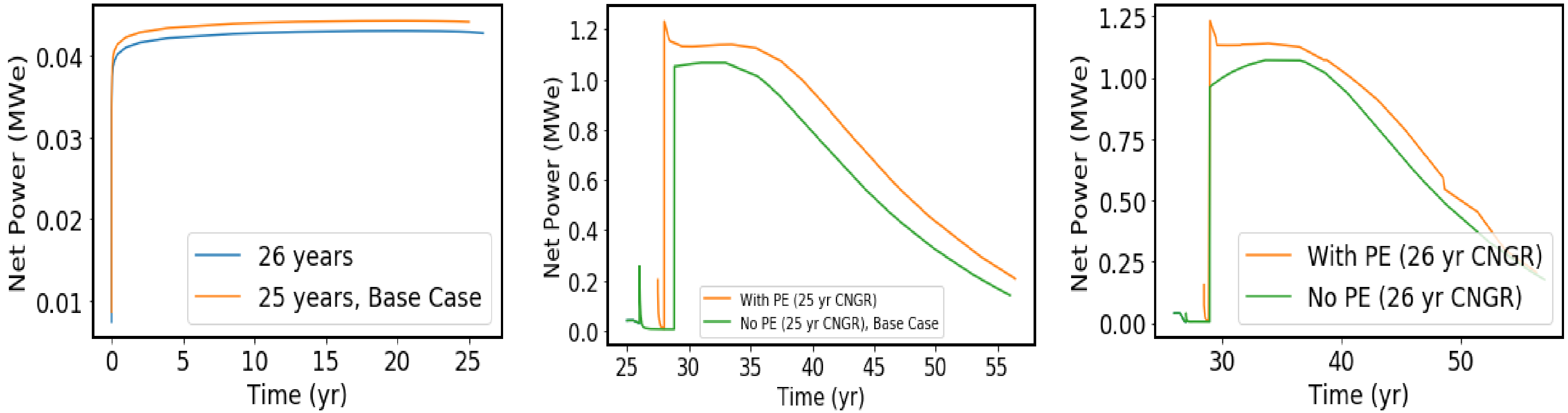

Figure A.2: Simulation results (time-series plots) for the 4 reservoir model example cases, showing the net geothermal power generated during the CNGR stage (0 – 25/26 years) and EGR-CPG stages (25/26 – 55/56 years).

Preprints (www.preprints.org) | NOT PEER-REVIEWED | Posted: 13 September 2021 doi:10.20944/preprints202109.0203.v1

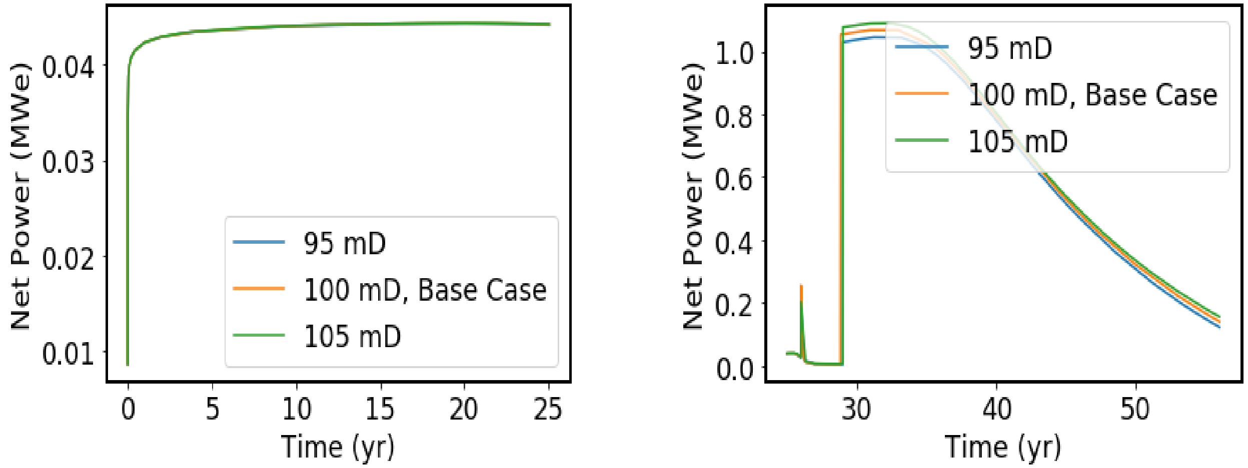

Figure A.3: Simulation results (time-series plots) for the reservoir permeability parameter, showing the geothermal net power generated during the CNGR stage (0 – 25 years) and EGR-CPG stages (25 – 55 years).

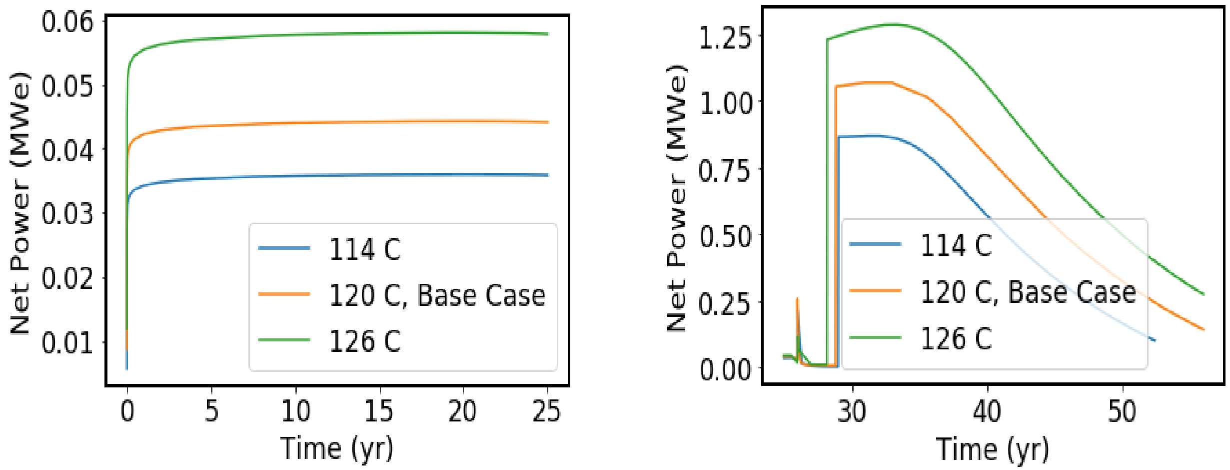

Figure A.4: Simulation results (time-series plots) for the reservoir temperature parameter, showing the geothermal net power generated during the CNGR stage (0 – 25 years) and EGR-CPG stages (25 – 55 years).

Preprints (www.preprints.org) | NOT PEER-REVIEWED | Posted: 13 September 2021 doi:10.20944/preprints202109.0203.v1

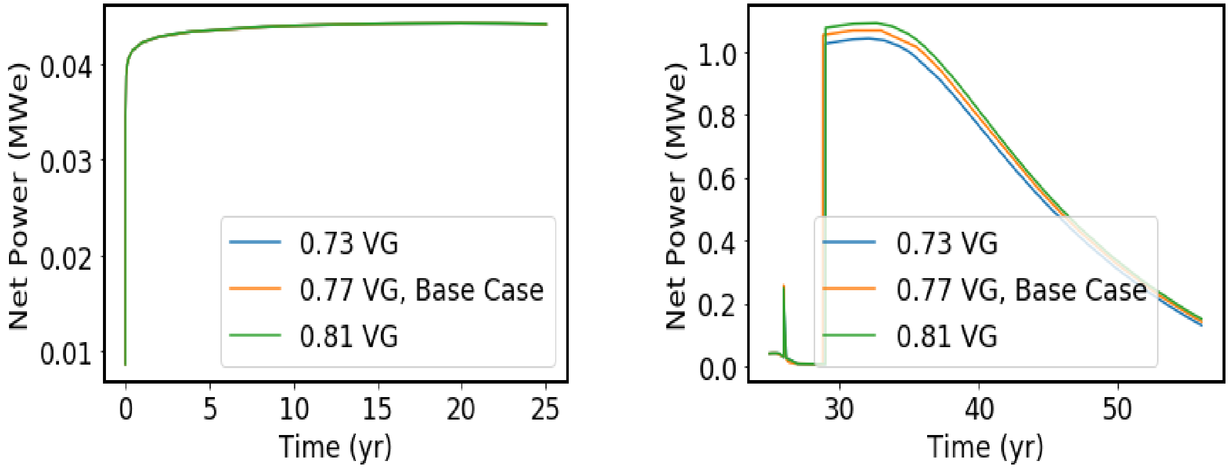

Figure A.5: Simulation results (time-series plots) for the relative permeability (van Genuchten) parameter, showing the geothermal net power generated during the CNGR stage (0 – 25 years) and EGR-CPG stages (25 – 55 years).

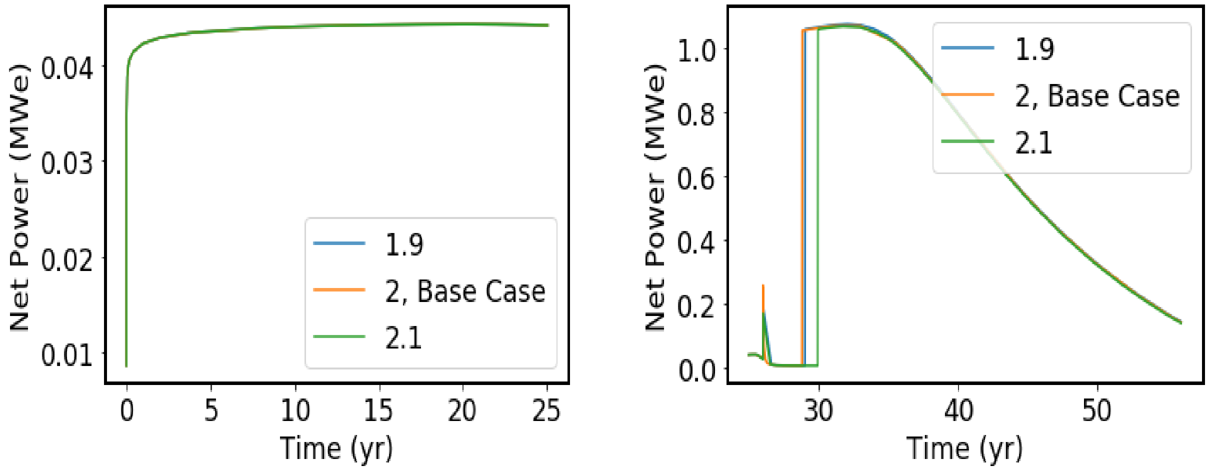

Figure A.6: Simulation results (time-series plots) for the reservoir permeability anisotropy parameter, showing the geothermal net power generated during the CNGR stage (0 – 25 years) and EGR-CPG stages (25 – 55 years).

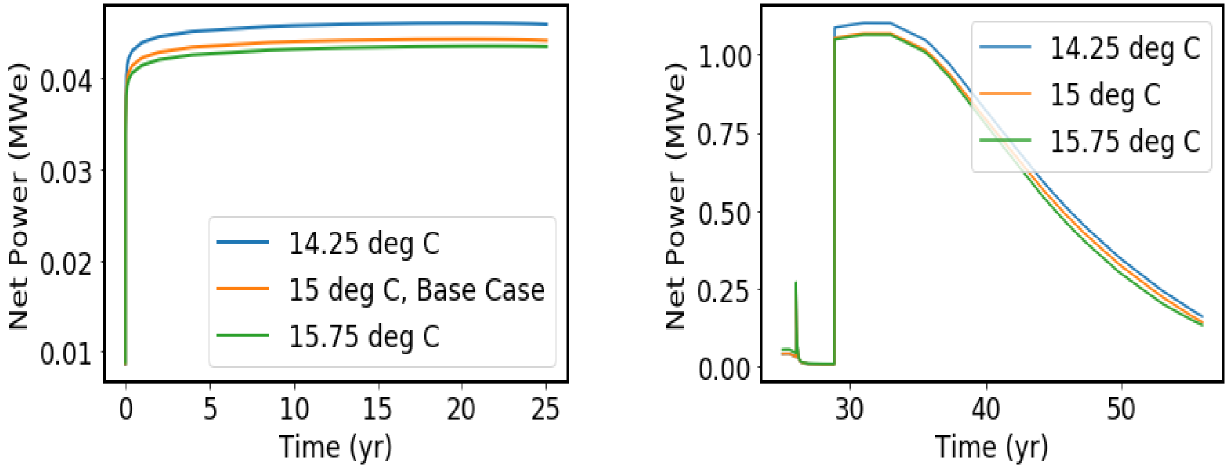

Figure A.7: Simulation results (time-series plots) for the mean ambient surface temperature parameter, showing the geothermal net power generated during the CNGR stage (0 – 25 years) and EGR-CPG stages (25 – 55 years).

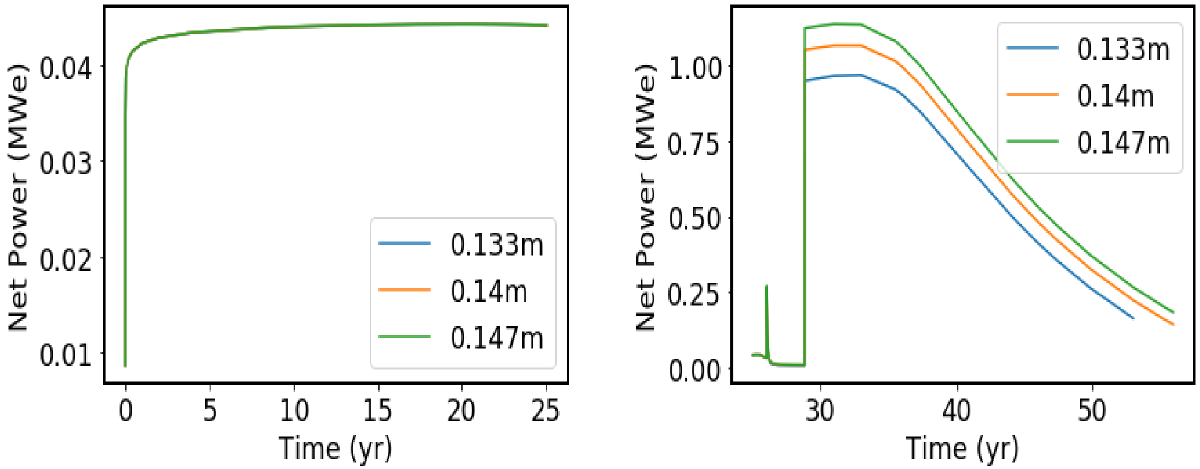

Figure A.8: Simulation results (time-series plots) for the well pipe diameter, showing the geothermal net power generated during the CNGR stage (0 – 25 years) and EGR-CPG stages (25 – 55 years).